View metadata, citation and similar papers at core.ac.uk

brought to you by CORE

provided by DigitalCommons@The Texas Medical Center

JOURNAL OF VIROLOGY, June 2009, p. 5321–5328 Vol. 83, No. 11
0022-538X/09/$08.00+0 doi:10.1128/JVI.02502-08
Copyright © 2009, American Society for Microbiology. All Rights Reserved.

# Prion Protein Glycosylation Is Not Required for Strain-Specific Neurotropism▽†

Justin R. Piro,[1] Brent T. Harris,[2] Koren Nishina,[1] Claudio Soto,[3] Rodrigo Morales,[3] Judy R. Rees,[4] and Surachai Supattapone[1,5]*

*Departments of Biochemistry,[1] Pathology,[2] Community and Family Medicine (Biostatistics and Epidemiology),[4] and Medicine,[5] Dartmouth Medical School, Hanover, New Hampshire 03755, and Department of Neurology, University of Texas Medical School, Houston, Texas 77030[3]*

Received 5 December 2008/Accepted 9 March 2009

**In this study, we tested the hypothesis that the glycosylation of the pathogenic isoform of the prion protein ($PrP^{Sc}$) might encode the selective neurotropism of prion strains. We prepared unglycosylated cellular prion protein ($PrP^{C}$) substrate molecules from normal mouse brain by treatment with PNGase F and used reconstituted serial protein cyclic misfolding amplification reactions to produce RML and 301C mouse prions containing unglycosylated $PrP^{Sc}$ molecules. Both RML- and 301C-derived prions containing unglycosylated $PrP^{Sc}$ molecules were infectious to wild-type mice, and neuropathological analysis showed that mice inoculated with these samples maintained strain-specific patterns of $PrP^{Sc}$ deposition and neuronal vacuolation. These results show that $PrP^{Sc}$ glycosylation is not necessary for strain-dependent prion neurotropism.**

Prion diseases are fatal neurodegenerative illnesses that occur in genetic, sporadic, and infectious forms (18). A critical pathogenic event common to the sporadic and infectious forms of prion disease is the misfolding of a host-encoded prion protein ($PrP^{C}$) into a pathogenic isoform ($PrP^{Sc}$). Infectious wild-type prions have been produced de novo from purified $PrP^{C}$, lipid, and synthetic poly(A) RNA molecules (13), confirming the proposition that the infectious agent lacks replicating nucleic acids (28). However, it remains unknown whether native mammalian prions contain only $PrP^{Sc}$ molecules, as proposed by the "protein-only" hypothesis or, alternatively, whether the maintenance of an infectious conformation might require a physical interaction between $PrP^{Sc}$ molecules and structural cofactors such as polyanions (12, 17).

Interestingly, prions can exist as distinct "strains" characterized by unique clinical features and patterns of neurotropism that are faithfully recapitulated upon serial passage within the same animal species (3, 4). Studies with yeast models and recombinant proteins indicate that prion proteins can adopt multiple, self-propagating conformations (19, 20, 24, 33, 34). However, it is difficult to explain the selective and self-propagating neurotropism of native mammalian prion strains on the basis of differential PrP polypeptide folding alone, and it remains unknown how neurons from different brain regions discriminate between different prion strains (11).

Mature PrP molecules have two N-linked glycosylation sites at residues 180 and 196 and therefore can be di-, mono-, or unglycosylated (14, 22). Interestingly, different ratios of $PrP^{C}$ glycoforms are found in different brain regions (2, 10, 32), and different prion strains produce distinctive ratios of $PrP^{Sc}$ glycoforms upon serial passage (9). Studies of transgenic mice show that $PrP^{C}$ glycosylation influences patterns of prion neurotropism in a strain-dependent manner (11, 35). Studies with human brain specimens have shown that the regional distribution of $PrP^{Sc}$ glycoforms is heterogenous in the sporadic but not the variant form of Creutzfeldt-Jakob disease (21). Taken together, these observations suggest the possibility that various patterns of $PrP^{Sc}$ glycosylation may direct the regional neurotropism of prion strains. However, technical difficulties in manipulating $PrP^{Sc}$ glycosylation have thus far precluded direct experimental testing of this hypothesis.

A series of recent advances has provided a new opportunity to produce infectious unglycosylated $PrP^{Sc}$ molecules in vitro by using serial protein misfolding cyclic amplification (sPMCA) reactions (7, 26), a cell-free prion amplification technique that faithfully preserves the strain properties of the initial seed material (6). Here, we use reconstituted sPMCA reactions to produce unglycosylated $PrP^{Sc}$ molecules derived from two mouse prion strains associated with easily distinguishable patterns of neurotropism (6). Neuropathological analysis of animals infected with these inocula shows that $PrP^{Sc}$ glycosylation is not required for the maintenance of strain-specific neurotropisms.

## MATERIALS AND METHODS

**Reagents.** Mouse prion stain RML was kindly provided by Stanley Prusiner (University of California, San Francisco). Mouse prion strain 301C was generated by serially passaging an isolate of bovine spongiform encephalopathy prions through C57BL mice. Mice used in inoculation experiments were female, C57BL6, aged 35 days, and purchased from Charles River (Wilmington, MA). $Prnp^{0/0}$ mice were kindly provided by David Harris (Washington University, St. Louis, MO) with permission from Charles Weissmann (Scripps Florida, Jupiter, FL). Immunoglobulin G monoclonal antibody (MAb) 27/33 was raised against purified recombinant mouse PrP 90-231 (kindly provided by Ilia Baskakov, University of Maryland Biotechnology Institute, Baltimore, MD) and subsequently purified from hybridoma cells by Bio Express (West Lebanon, NH). Noninfectious mouse brains were purchased from BioChemed (Winchester, VA). These

* Corresponding author. Mailing address: Department of Biochemistry, 7200 Vail Building, Dartmouth Medical School, Hanover, NH 03755. Phone: (603) 650-1192. Fax: (603) 650-1193. E-mail: supattapone@dartmouth.edu.

† Supplemental material for this article may be found at http://jvi.asm.org/.

▽ Published ahead of print on 18 March 2009.

brains were from CD1 mice, both sexes, aged 15 weeks, and were immediately snap-frozen in liquid nitrogen after removal.

**Preparation of brain homogenates.** In several instances, brain homogenates were used either directly as inocula or as reagents for PMCA reactions; they were prepared as follows. One mouse brain (normal, $Prnp^{0/0}$, RML infected, or 301C infected) weighing ~0.5 g was homogenized using either a Potter homogenizer (for normal brains) or a disposable plastic homogenizer (VWR Scientific, Boston, MA) (for infected brains) in 5 ml of cold phosphate-buffered saline (PBS) (without calcium or magnesium). The resulting 10% (wt/vol) homogenate was then centrifuged at 200 × *g* for 30 s, and the supernatant was collected and frozen at −80°C.

**Purification of native and unglycosylated $PrP^C$.** Unglycosylated $PrP^C$ was purified as previously described (26). Briefly, 12 mouse brains were Potter homogenized in 40 ml of cold buffer A (20 mM MOPS [morpholinepropanesulfonic acid] [pH 7.0] and 150 mM NaCl) with Complete EDTA-free protease inhibitor (Roche, Indianapolis, IN). The homogenate was centrifuged at 200 × *g* for 30 s, and the supernatant was removed and centrifuged again at 3,200 × *g* for 20 min. The resulting pellet was resuspended using a Dounce homogenizer in 30 ml of cold buffer A with Complete EDTA-free protease inhibitor. Four milliliters of 10% deoxycholate–Triton X-100 detergent was added, and the mixture was incubated on ice for 30 min. After solubilization, the homogenate was centrifuged at 100,000 × *g* for 30 min. The supernatant was then added to a preequilibrated 2-ml immobilized metal ion affinity chromatography-$CuSO_4$ column (GE Healthcare, Piscataway, NJ). The column was washed with 10 ml of wash buffer (10 mM imidazole in buffer A [pH 7.0] and 0.5% Triton X-100), and eluted with 10 ml elution buffer (20 mM MES [morpholineethanesulfonic acid] [pH 6.4], 150 mM imidazole in buffer A [pH 7.0], 150 mM NaCl, and 1% Triton X-100). Next, the eluate was applied to a preequilibrated 2-ml SP Sepharose cation exchange column (Sigma, St. Louis, MO). The SP column was washed with 10 ml of SP wash buffer (20 mM MOPS [pH 7.0], 250 mM NaCl, and 0.5% Triton X-100) and eluted in 8 ml of SP elution buffer (20 mM MOPS [pH 7.5], 500 mM NaCl, and 0.5% Triton X-100). The resulting eluate was designated the "native" preparation. To remove the N-linked glycans from $PrP^C$, 50 μl (~25,000 units) glycerol-free peptide *N*-glycosidase F (PNGase F) (New England Biolabs, Beverly, MA) was added to 500 μl of the SP eluate. This mixture was then incubated for 24 h at 37°C. After this initial incubation, another 50 μl of PNGase F was added to the tube and incubated for another 24 h at 37°C. To repurify deglycosylated $PrP^C$, the sample was mixed with 200 μl immobilized metal ion affinity chromatography-$CuSO_4$ resin and incubated with end-over-end rotation for 30 min at 4°C. The protein-resin slurry was poured into a column support and washed with 20 ml of wash buffer followed by elution with 500 μl of elution buffer. The eluate was put into a 3,500-molecular-weight-cutoff Slide-A-Lyser (Pierce, Rockford, IL) and dialyzed overnight into buffer C (20 mM MOPS [pH 7.5], 150 mM NaCl, and 0.5% Triton X-100). The final sample was termed unglycosylated $PrP^C$ substrate.

**sPMCA.** Serial prion propagation using sPMCA was performed using a method described previously by Castilla et al. (7). To avoid cross-contamination, only one strain was used within the sonicator at a time. Also, as a precautionary measure to minimize the possibility of residual contamination between different runs (which can be caused by tube leakage during PMCA), the microplate cup horn was decontaminated between strains by soaking in 100% household bleach (60,000 ppm sodium hypochlorite) for 5 min with one 30-s pulse and then rinsed with deionized, filtered $H_2O$. Furthermore, all strain work was carried out in laminar-flow biosafety cabinets with disposable surfaces and aerosol barrier tips. To produce substrate mixtures for normal brain homogenate or $Prnp^{0/0}$ "ablated" brain homogenate sPMCA (Abl-sPMCA) reactions, 75 μl of 10% normal mouse brain homogenate or 10% ablated brain homogenate (homogenate from $Prnp^{0/0}$ mice) was mixed with 15 μl of TEI (3.33% Triton X-100, 33.33 mM EDTA, 333.33 mM imidazole [pH 8.0]). On the first day, 10 μl of 10% brain homogenate from RML- or 301C-infected animals was diluted 1:100 in PBS and added to a 0.5-ml thin-walled PCR tube. Reaction tubes were subjected to PMCA for 24 h using a Misonix s3000 programmable sonicator equipped with a microplate horn (Misonix, Farmingdale, NY) containing 350 ml of water. The sonicator was set to deliver 30-s bursts every 30 min at output 6.5. Temperature within the microplate horn was maintained by flowing heated water through aluminum coils surrounding the horn. Sample tubes were mounted in a holder that prevents lid opening and holds tubes ~3 mm from the horn surface. After 24 h, the tubes were removed from the sonicator, and 10 μl of the reaction mixture volume was added to a new tube containing fresh substrate. This was carried out for 15 consecutive cycles, effectively diluting the original inoculum $10^{15}$-fold. To produce substrate mixtures for native and unglycosylated $PrP^C$ sPMCA reactions, 37.5 μl of either native or unglycosylated $PrP^C$ preparations (prepared as described above) was mixed with 25 μl of 10% ablated brain homogenate, 15 μl of TEI, and 12.5 μl of buffer B (20 mM MOPS [pH 7.5], 150 mM NaCl, 1% Triton X-100). On the first day, 10 μl of 10% brain homogenate from RML- or 301C-infected animals diluted 1:100 in PBS was added to the reaction tube. Tubes were subjected to the same sonicator settings described above. After 24 h, 10 μl of the reaction mixture was added to a new tube containing fresh substrate. This was carried out for a total of 15 days.

**Preparation of inocula.** For each sPMCA-generated inoculum, five tubes containing 200 μl reaction mixture/tube were prepared. Each tube was spiked with 20 μl of material from the day 15 tube of that group (prepared as described above). These tubes were subjected to 48 h of sonication at the settings described above. The five samples in each group were pooled together and centrifuged at 200 × *g* for 30 s. The supernatant was transferred to a new tube and centrifuged again at 200 × *g* for 30 s. The supernatant was transferred to a new tube and passed through a 25-gauge needle five times, followed by passage through a 28-gauge needle five times. The material was then centrifuged at 100,000 × *g* for 1 h at 4°C. The supernatant was removed, and the pellet was resuspended in 500 μl PBS containing 1% Triton X-100. This material was then sequentially passed through increasing-gauge needles (18, 23, 25, and 28 gauge) five times each. An aliquot of the resuspended material was analyzed for $PrP^{Sc}$ content by Western blotting. Another aliquot was diluted 1:10 into PBS plus 5 mg/ml bovine serum albumin to prepare the inoculum samples. For brain-derived inocula, 100 μl of 10% (wt/vol) prion-infected brain homogenate was diluted 1:10 into PBS plus 5 mg/ml bovine serum albumin.

**Scrapie inoculation and diagnosis.** To avoid contamination, inoculations of groups from different strains were performed on separate days in laminar-flow biosafety cabinets using disposable syringes, gloves, and surfaces. Intracerebral inoculations were performed using 28-gauge hypodermic needles inserted into the parietal lobe. Each animal received 30 μl of inocula. After inoculation, mice were examined daily by veterinary staff blinded to the experimental groups. Standard diagnostic criteria were used to identify animals showing signs of scrapie (5, 29).

**Neuropathology.** Animals whose deaths were imminent were euthanized by $CO_2$ inhalation, and their brains were removed quickly using sterile-packaged dissection instruments on disposable surfaces to avoid cross-contamination. Brains were fixed by immersion in 10% buffered formalin for up to 1 week. Brains were then sectioned in the sagittal and parasagittal planes at ~2- to 3-mm intervals and placed into tissue-processing cassettes. The cassettes were immersed into 90% formic acid for 60 to 90 min and then placed in 10% formalin. Tissue was then embedded in paraffin and cut into 4-μm sections. These sections were then stained with hematoxylin and eosin or anti-PrP antibody (immunohistochemistry [IHC]). A single neuropathologist, who was blinded to the experimental groups, examined all of the slides. Each brain was scored for the degree of vacuolation in six different brain regions: parietal cortical layers 1 and 2, layers 3 and 4, and layers 5 and 6; hippocampus; cerebellum; and brain stem. Scoring was performed using ordinal variables as previously described (7, 16): 0, no lesions; 0.5, minimum vacuolation (two to three vacuoles in half a 40× objective field); 1.0, little vacuolation (three to five vacuoles in half a field); 2.0, moderate vacuolation (several vacuoles evenly scattered); 3.0, extensive vacuolation (many vacuoles distributed in half a field); 4.0, severe vacuolation (numerous vacuoles often coalescing). Slides from adjacent sections were also prepared for antigen retrieval using CitraPlus reagent (Biogenex, San Ramon, CA) (pH 6.23) and pressure steaming to 126°C (16 $lb/in^2$), followed by immunostaining with MAb 27/33 (final working concentrations, 3 μg/ml) by using a Biogenix i6000 automated stainer. Immunodeposition was visualized by using a horseradish peroxidase–3,3′-diaminobenzidine MultiLink detection kit (Biogenex) according to the manufacturer's recommended protocol. Each brain was scored for anti-PrP immunodeposition as follows: 0, no deposition; 1.0, minimal deposition; 2.0, moderate deposition; 3.0, extensive deposition.

**$PrP^{Sc}$ detection.** All protease-digested samples (with proteinase K) were incubated with 25 μg/ml proteinase K for 30 min at 37°C with shaking at 800 rpm in an Eppendorf Thermomixer (Fisher Scientific, Pittsburgh, PA). An equal volume of 2× sodium dodecyl sulfate (SDS) sample buffer was added, and samples were boiled for 10 min at 95°C. SDS-polyacrylamide gel electrophoresis (PAGE) was then performed using 1.5-mm 12% polyacrylamide gels with an acrylamide/bisacrylamide ratio of 29:1. The gel was then transferred to a methanol-charged polyvinylidene difluoride membrane (Millipore, Billerica, MA) using a Transblot SD semidry transfer cell (Bio-Rad, Hercules, CA). The transfer was set at 2 $mA/cm^2$ for 30 min. To visualize PrP signals, the membrane was incubated in Hood skim milk (Chelsea, MA) buffered with TBST (10 mM Tris [pH 7.1], 150 mM NaCl, 0.1% Tween 20). The blocked membrane was then incubated overnight at 4°C with 27/33 and diluted 1:25,000 (0.12-μg/ml final concentration). The membrane was then washed three times for 10 min in TBST. Last, the membrane was incubated for 1 h with horseradish peroxidase-labeled

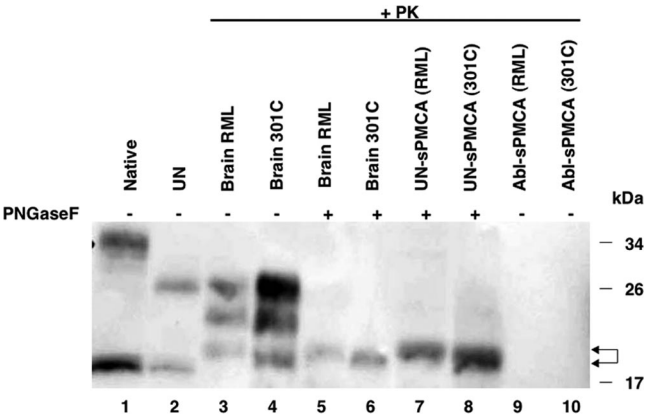


FIG. 1. Western blot showing samples of inocula. Lanes 1 and 2 show nondigested $PrP^C$ used as a substrates in sPMCA reactions. Strong reactivity against the ~18-kDa C1 proteolytic fragment (37) is characteristic of primary MAb 27/33 used to develop this Western blot. The remaining samples were subjected to limited proteolysis with proteinase K (+PK). Some proteolyzed samples were also deglycosylated by treatment with PNGase F (~5,000 units) prior to SDS-PAGE, as indicated. The bracket indicates a strain-specific difference in electrophoretic mobility between unglycosylated $PrP^{Sc}$ bands derived from strains 301C and RML.

anti-mouse immunoglobulin G secondary antibody conjugate (GE Healthcare) diluted 1:5,000 in TBST. Again, the membrane was washed four times for 10 min each in TBST. Blots were developed with West Femto (Pierce, Rockford, IL) chemiluminescence substrate, and images were captured digitally using a Fuji (Fujifilm, Tokyo, Japan) LAS-3000 chemiluminescence documentation system. Relative molecular masses were determined by comparison to prestained standards from Fermentas (Hanover, MD). Digitally captured images of Western blots were subjected to densitometric analysis using the program Image Gauge v. 4.22 (Fuji). For each signal, replicate measurements were obtained ($n = 3$), and values were averaged.

**Enzymatic deglycosylation.** To deglycosylate $PrP^{Sc}$ molecules, 100 μl of each sample was protease digested as described above. To inactivate proteinase K, phenylmethylsulfonyl fluoride dissolved in ethanol was added to each sample for a final concentration of 1 mM. Samples were then diluted to 750 μl in PBS and 10% Sarkosyl (Sigma) and centrifuged at 100,000 × *g* for 1 h at 4°C. Supernatants were removed, and pellets were resuspended into 100 μl of 1× glycoprotein denaturing buffer (New England Biolabs) and boiled for 10 min at 95°C. Next, 11 μl of 10× G7 reaction buffer and 11 μl of 10% NP-40 (both from New England Biolabs) were added to the reaction tubes and mixed. Ten microliters of PNGase F enzyme (~5,000 units) was then added to the tubes and incubated overnight at 37°C. To stop the reaction, an equal volume of 2× SDS sample buffer was added to each tube and boiled for 10 min at 95°C.

**Urea denaturation assay.** Samples containing 8% (wt/vol) brain homogenate in PBS without calcium or magnesium plus 2% Triton were indirectly sonicated using a Misonix 3000-MPD programmable sonicator equipped with a microplate horn at power 7.5 for 30 s. Following sonication, 10-μl samples were diluted 1:4 with various aqueous solutions to achieve final urea concentrations of 0, 1, 2, 3, 4, 5, and 6 M. Adjusted samples were incubated at 50°C for 3 h with shaking at 800 rpm in a Thermomixer apparatus (Eppendorf, Westbury, NY). After incubation, 80 μl of PBS–1% Triton X-100 containing 60 μg/ml proteinase K was added to each tube, and samples were incubated for 1 h at 37°C with shaking in a Thermomixer apparatus. After digestion, 40 μl of 4× SDS sample buffer was added to each tube, and the sample was boiled for 10 min. Quantified Western blot signals were best fitted using a sigmoidal dose-response equation with a variable slope using the program Prism 5.0a (GraphPad Software, La Jolla, CA).

## RESULTS

To produce unglycosylated sPMCA (UN-sPMCA) inocula, we performed 16 rounds of reconstituted sPMCA reactions using enzymatically deglycosylated mouse $PrP^C$ as a substrate and mouse prion strains RML and 301C as seeds in the first round. Western blot analysis confirmed the presence of protease-resistant $PrP^{Sc}$ molecules in the final (round 16) UN-sPMCA samples for both strains (Fig. 1, lanes 7 and 8). Interestingly, the UN-sPMCA(301C) product exhibited slightly slower mobility by SDS-PAGE following proteinase K digestion than the UN-sPMCA(RML) product, corresponding to the similar ~2-kDa difference observed between these two strains in the migrations of their proteinase K-digested, PNGase F-treated brain-derived $PrP^{Sc}$ molecules (Fig. 1, compare lanes 7 and 8 with lanes 5 and 6) (6). This observation indicates that the strain-specific, conformation-dependent biochemical property of electrophoretic mobility following proteinase K digestion appears to be preserved during sPMCA propagation using unglycosylated $PrP^C$ substrate. Control samples in which the initial input seed for each prion strain was serially diluted and mock propagated in the absence of $PrP^C$ substrate (Abl-sPMCA) yielded no detectable $PrP^{Sc}$ molecules by Western blotting (Fig. 1, lanes 9 and 10).

We injected normal C57BL mice intracerebrally with brain-derived RML, 301C, or the final-day products of 16 round sPMCA reactions originally seeded with these prion strains. Whereas mice inoculated with brain-derived prions or the day 16 products of sPMCA reactions using unglycosylated $PrP^C$ substrate developed clinical prion disease with incubation times ranging from ~170 to ~350 days, mice inoculated with the day 16 products of negative control sPMCA reactions lacking $PrP^C$ substrate (Abl-sPMCA) remained healthy >400 days after inoculation (Table 1). It is worth noting that the concentration of $PrP^{Sc}$ is ~40-fold greater in the brain-derived inocula than in the UN-sPMCA inocula, and therefore, it is difficult to interpret the differences in prion incubation times between those groups.

Western blot analysis confirmed the presence of protease-resistant $PrP^{Sc}$ molecules in the brains of mice from each group with clinically diagnosed prion disease (Fig. 2). Di-, mono-, and unglycosylated $PrP^{Sc}$ molecules were all present in the brains of mice infected with UN-sPMCA(301C) and UN-sPMCA(RML) inocula that contained only unglycosylated $PrP^{Sc}$ molecules (Fig. 2, lanes 9 and 10); these results are similar to and consistent with those previously reported by Tuzi et al., in which an inoculum containing unglycosylated $PrP^{Sc}$ molecules originally derived from mouse prion strain 79A was infectious to wild-type mice and all three $PrP^{Sc}$ glycoforms were present in the brains of recipient mice (35).

TABLE 1. Prion incubation times in wild-type mice inoculated intracerebrally with brain-derived and sPMCA-generated prions

| Inoculum | No. of infected mice/total no. of mice | Mean incubation time (days) ± SEM |
|---|---|---|
| Brain RML | 5/5 | 169 ± 2 |
| Brain 301C | 9/9 | 193 ± 1 |
| UN-sPMCA(RML) | 13/13 | 202 ± 2 |
| UN-sPMCA(301C) | 6/7 | 348 ± 26[a] |
| Abl-sPMCA(RML) | 0/8 | >407 |
| Abl-sPMCA(301C) | 0/8 | >407 |
| Homog-sPMCA(301C) | 8/8 | 265 ± 63 |
| Native sPMCA(301C) | 8/8 | 237 ± 32 |

[a] Ongoing experiment.

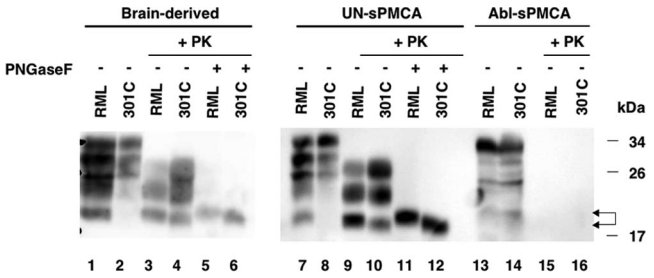


FIG. 2. Western blot showing representative brain homogenates from inoculated animals. Where indicated, samples were subjected to limited proteolysis or deglycosylated by treatment with PNGase F (~5,000 units). The bracket indicates a strain-specific difference in electrophoretic mobility between unglycosylated $PrP^{Sc}$ bands derived from strains 301C and RML. The segment of the blot containing lanes 1 to 6 was exposed for 1 min, and the segment containing lanes 7 to 16 was exposed for 8 min. +PK, with proteinase K treatment.

The brains of mice inoculated with either brain-derived RML or UN-sPMCA(RML) prions contained a comparatively even distribution of the three $PrP^{Sc}$ glycoforms (Fig. 2, lanes 3 and 9), whereas diglycosylated $PrP^{Sc}$ appeared to be relatively enriched in the brains of mice inoculated with either brain-derived 301C or UN-sPMCA(301C) prions (Fig. 2, lanes 4 and 10). Densitometric quantification of the ratios of deglycosylated:unglycosylated $PrP^{Sc}$ molecules on unsaturated Western blot images yielded values of 0.7 and 0.6 for the brain-derived RML and UN-sPMCA(RML) samples, respectively, and 1.6 and 1.8 for the brain-derived 301C and UN-SPMCA(301C) samples, respectively. Furthermore, enzymatic deglycosylation revealed that the proteinase K-resistant $PrP^{Sc}$ bands in samples from mice inoculated with either brain-derived 301C or UN-sPMCA(301C) prions migrated ~2 kDa more rapidly than the corresponding bands in samples from mice inoculated with either brain-derived RML or UN-sPMCA(RML) prions (Fig. 2, lanes 5, 6, 11, and 12). Another feature preserved in the brains of animals inoculated with brain-derived 301C and UN-sPMCA(301C) prions is the lack of the ~19-kDa calpain-generated C2 fragment (40), which can be appreciated for samples from animals inoculated with brain-derived RML and UN-sPMCA(RML) prions that were treated with proteinase K (Fig. 2, compare lanes 2 and 8 to lanes 1 and 7). A urea denaturation assay revealed that $PrP^{Sc}$ molecules in animals inoculated with either brain-derived RML or UN-sPMCA(RML) prions (half-maximal denaturation concentration for both groups of ~3.5 M urea) were significantly more stable than $PrP^{Sc}$ molecules in animals inoculated with either brain-derived 301C or UN-sPMCA(301C) prions (half-maximal denaturation concentration for both groups of ~2.5 M urea) (see Fig. S1 in the supplemental material). Taken together, these results indicate that several biochemical properties of the prion strains analyzed (i.e., $PrP^{Sc}$ glycosylation profile, electrophoretic mobility following proteinase K digestion, and the presence of a detectable C2 proteolytic fragment) were preserved in vivo by the sPMCA-generated unglycosylated $PrP^{Sc}$ molecules. As expected, no $PrP^{Sc}$ molecules were detected in the brains of age-matched, clinically well-appearing mice that had been inoculated with Abl-sPMCA(301C) and Abl-sPMCA(RML) products (Fig. 2, lanes 15 and 16), consistent with the lack of prion infectivity in those control samples. Additional control experiments showed that $PrP^{Sc}$ molecules in the brains of mice inoculated with sPMCA products of reactions using crude brain homogenate (Homog-sPMCA) or reconstituted native $PrP^{C}$ substrates (native sPMCA) also retained their strain-specific patterns of electrophoretic mobility (see Fig. S2 in the supplemental material).

Microscopic analysis of the neuropathology of prion-infected mice in each of the experimental groups (i.e., inoculated with brain-derived or UN-sPMCA prions) revealed spongiform degeneration, PrP immunodeposition, and reactive astrogliosis, whereas the brains of mice infected with Abl-sPMCA control inocula lacked all of these characteristics (Fig. 3). Within the cerebral cortex of RML-infected animals, both vacuolation and PrP immunodeposition could be better appreci-

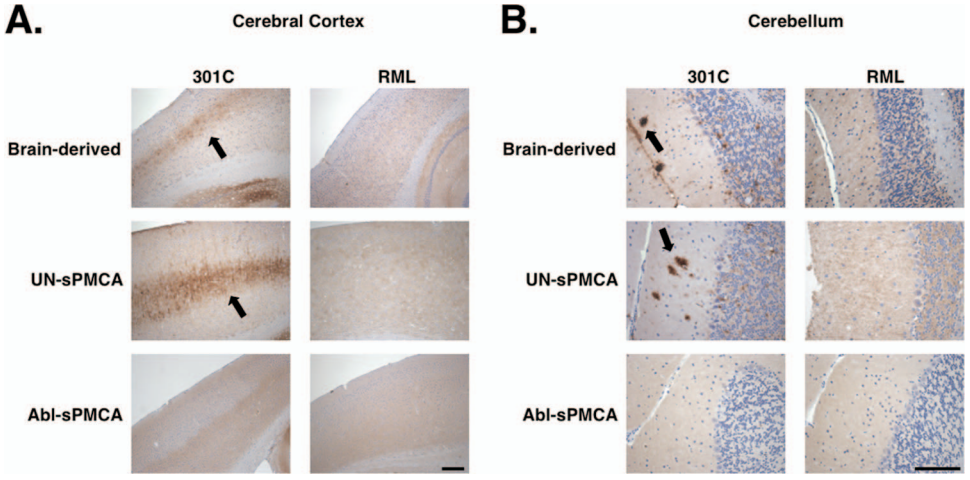


FIG. 3. Representative histological fields of cerebral cortex and cerebellum. Shown is PrP immunohistochemical staining from animals injected with brain-derived or sPMCA-generated 301C and RML prions. (Top) Animals injected with brain-derived prions. (Middle) Animals injected with UN-sPMCA prions. (Bottom) Control animals injected with Abl-sPMCA. (A) Cerebral cortex. Arrows indicate the location of strain-specific staining within layers 3 and 4 of the cerebral cortex. Scale bar, 200 μm. (B) Cerebellum. Arrows indicate the location of PrP aggregates. Scale bar, 100 μm.

ated at a higher magnification (see Fig. S3 in the supplemental material). Strikingly, PrP immunodeposition in the cerebral cortex of mice inoculated with either brain-derived 301C or UN-sPMCA(301C) prions appeared to be highly concentrated in layers 3 and 4, whereas PrP immunodeposition appeared to be evenly distributed throughout all six cortical layers in mice inoculated with either brain-derived RML or UN-sPMCA(RML) prions (Fig. 3A). Furthermore, there appeared to be many discrete ~1- to 30-μm PrP aggregates in the cerebellum of mice inoculated with either brain-derived 301C or UN-sPMCA(301C) prions, whereas no aggregates larger than 2 μm could be seen in the cerebellum of mice inoculated with either brain-derived RML or UN-sPMCA(RML) prions, and PrP immunodeposition appeared to be diffusely distributed throughout the cerebellar cortex in those animals (Fig. 3B). Taken together, these results indicate that characteristic patterns of PrP immunodeposition in the cerebral cortex and cerebellum, which are easily distinguishable between strains RML and 301C, are preserved by $PrP^{Sc}$ molecules lacking glycosylation. In additional control experiments, we also observed the concentration of PrP immunodeposition in cortical layers 3 and 4 and the presence of discrete cerebellar PrP aggregates in the brains of mice inoculated with sPMCA-propagated 301C prions using either normal mouse brain homogenate or partially purified $PrP^{C}$ reconstituted with $Prnp^{0/0}$ brain homogenate (native) as a substrate, confirming that neither the sPMCA technique itself nor the reconstitution of partially purified $PrP^{C}$ molecules with $Prnp^{0/0}$ brain homogenate influences the ability of $PrP^{Sc}$ molecules to propagate and encode these distinctive neurotropic features (see Fig. S4 in the supplemental material).

To compare the patterns of neurotropism in the various groups of prion-infected mice at a broader level, we compiled and analyzed regional profiles of PrP immunodeposition and neuronal vacuolation scores. The results showed that for both strains 301C (Fig. 4A and C) and RML (Fig. 4B and D), the regional profiles of PrP immunodeposition and vacuolation were similar for brain-derived and UN-sPMCA prions. The regional variations between the two strains were more easily distinguished by PrP immunodeposition (Fig. 4, compare A and B) than vacuolation (Fig. 4, compare C and D), primarily because the increased PrP deposition in layers 3 and 4 appeared not to be associated with increased levels of vacuolation in those layers. Taken together, these results indicate that the unglycosylated $PrP^{Sc}$ molecules can encode strain-specific regional patterns of $PrP^{Sc}$ accumulation. Data were analyzed using Stat 9.0 (Stata statistical software release 9.0; Stata Corporation, College Station, TX). For each of the experimental groups, we compared vacuolation and immunohistochemistry characteristics in all six brain regions using the Wilcoxon rank sum test. This statistical approach identified no significant differences in vacuolation between the brain-derived 301C and UN-sPMCA(301C) groups or in IHC staining between the brain-derived RML and the UN-sPMCA(RML) groups. Global differences in the absolute magnitudes of IHC staining between the brain-derived 301C and UN-sPMCA(301C) groups and of vacuolation between the brain-derived RML and the UN-sPMCA(RML) groups rendered these comparisons nonamenable to statistical analysis, but Fig. 4 shows that the patterns of these characteristics across brain regions also appear very similar in regional profile. As an additional control, we also examined the patterns of PrP deposition in animals infected with Homog-sPMCA(RML) and Homog-sPMCA(301C) inocula. As expected, the regional profiles of these groups were similar to those of the UN-sPMCA(RML) and UN-sPMCA(301C) groups, respectively (compare Fig. S5 in the supplemental material to Fig. 4A and B).

## DISCUSSION

In this study, we report for the first time that $PrP^{Sc}$ glycosylation is not required for the maintenance of strain-dependent prion neurotropism. A corollary of this result is that the selective neurotropism of mammalian prions must be encoded either by strain-specific differences in $PrP^{Sc}$ polypeptide conformation or by putative accessory molecules such as lipids or polyanions (13, 17, 38, 39).

The phenomenon of strain-specific neurotropism implies that neurons must be able to recognize and distinguish between different prion strains. The hypothesis, which our findings refute, that glycosylation might be the distinguishing feature of $PrP^{Sc}$ molecules recognized by cells was originally attractive for several reasons. First, the glycans are large surface-exposed structures that appear to be well positioned to mediate cell target interactions (41). Second, there is great diversity in PrP glycosylation, which could therefore provide a basis for diverse patterns of neuronal targeting (30). Third, some prion strains appear to be associated with distinctive $PrP^{Sc}$ glycoform patterns (9). Fourth, $PrP^{C}$ glycoform patterns vary in different brain regions (2, 10, 32) and in different neuronal populations (15), and it is conceivable that prions containing a specific ensemble of $PrP^{Sc}$ glycoforms might prefer to propagate in neurons with a similar ensemble of $PrP^{C}$ glycoforms. Finally, $PrP^{C}$ glycosylation influences both strain and cross-species susceptibility to prion infection (11, 27, 35).

Because nondenatured $PrP^{Sc}$ molecules purified from prion-infected brains are highly aggregated and resistant to enzymatic deglycosylation, it is not possible to generate fully deglycosylated $PrP^{Sc}$ molecules by directly treating samples of infectious prions with glycosidases. Recently, Castilla et al. showed that sPMCA could be used to propagate the characteristic phenotypic properties of several murine prion strains faithfully, including their specific patterns of neuronal targeting (6). For the purposes of this study, we utilized sPMCA to propagate two of these mouse-adapted prion strains with easily distinguishable patterns of neuronal targeting, RML and 301C. To prepare an appropriate sPMCA substrate, we used PNGase F to deglycosylate native mouse $PrP^{C}$ under nondenaturing conditions. Our previous studies showed that unglycosylated $PrP^{C}$ prepared in this manner is a competent and, indeed, necessary substrate for the in vitro propagation of mouse prions (26). Using this approach, we have been able to eliminate PrP glycosylation without the need to mutate the PrP sequence, thereby avoiding a perturbation that could potentially constrain the folding pathway of $PrP^{Sc}$ molecules during prion formation (25, 36).

Our neuropathological analysis revealed no observable differences between mice inoculated with glycosylated and mice inoculated with unglycosylated $PrP^{Sc}$ molecules. Two of the most striking strain-dependent neuropathological differences

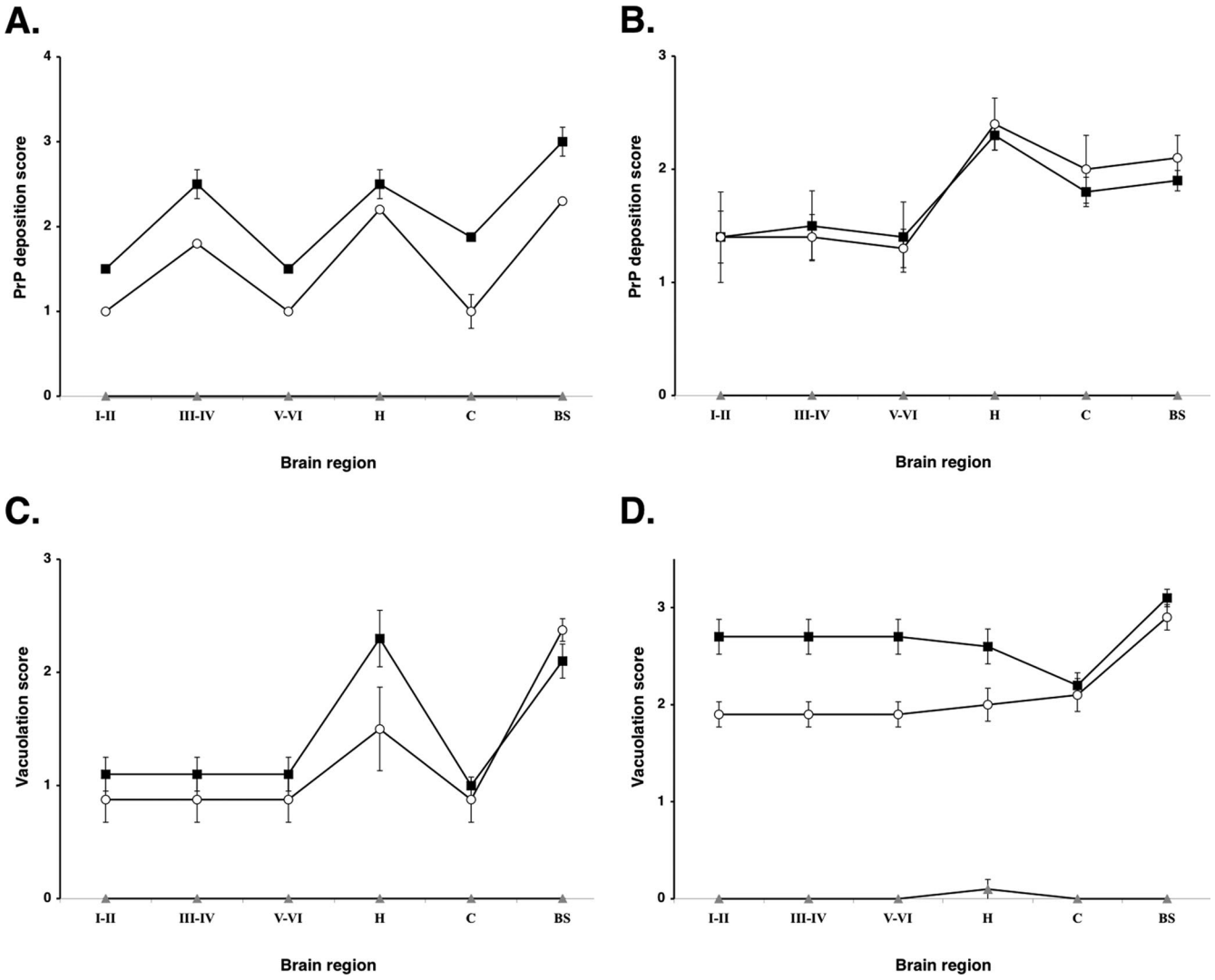


FIG. 4. Regional neuropathology of mice infected with brain-derived and sPMCA-generated inocula. (A) PrP immunohistochemistry profiles of animals inoculated with samples containing brain-derived 301C (■), UN-sPMCA(301C) (○), and Abl-sPMCA(301C) (▲). (B) PrP immunohistochemistry profiles of animals inoculated with samples containing brain-derived RML (■), UN-sPMCA(RML) (○), and Abl-sPMCA(RML) (▲). (C) Vacuolation profile scores of animals inoculated with samples containing brain-derived 301C (■), UN-sPMCA(301C) (○), and Abl-sPMCA(301C) (▲). (D) Vacuolation profile scores of animals inoculated with samples containing brain-derived RML (■), UN-sPMCA(RML) (○), and Abl-sPMCA(RML) (▲). Brain regions I and II, cerebral cortical layers 1 and 2; III and IV, cortical layers 3 and 4; V and VI; cortical layers 5 and 6; H, hippocampus; C, cerebellum; BS, brain stem. The mean values ($n$ = 4 to 9 animals/group) ± standard errors of the means are shown.

maintained by unglycosylated $PrP^{Sc}$ molecules were (i) $PrP^{Sc}$ deposition in layers 3 and 4 of the cerebral cortex in 301C-infected mice versus deposition throughout the entire thickness of the cortex in RML-infected mice and (ii) the appearance of punctate and larger $PrP^{Sc}$ aggregates in the cerebellum of 301C-infected mice versus a diffuse pattern of deposition in RML-infected mice. Thus, our data indicate that the lack of PrP glycosylation did not alter strain-specific neuronal targeting at either the cellular or regional level of the brain. Interestingly, another strain-dependent neuropathological feature that was preserved when animals were inoculated with unglycosylated $PrP^{Sc}$ molecules was the severity of vacuolation and PrP deposition in specific brain regions. This phenomenon was most noticeable in the cerebral cortex of RML-infected animals (Fig. 3; see Fig. S3 in the supplemental material). Further work is required to understand why prion strains cause different rates of $PrP^{Sc}$ deposition in specific brain regions.

As previously described by Tuzi et al., we observed that mice inoculated with unglycosylated $PrP^{Sc}$ molecules produced prions containing both glycosylated and unglycosylated PrP molecules (35). Furthermore, we found that the resulting $PrP^{Sc}$ molecules appeared to maintain strain-dependent patterns of electrophoretic mobility following cleavage with proteinase K. Since the precise location of proteinase K cleavage is most likely determined by the core conformation of $PrP^{Sc}$, this observation suggests that $PrP^{Sc}$ glycosylation is also unnecessary for the maintenance of strain-specific differences in $PrP^{Sc}$ conformations between RML and 301C during passage in animals.

The cellular mechanism that underlies strain-dependent prion neurotropism is currently unknown, but several possibilities exist. First, different neuronal subpopulations might possess different sets of recognition sites, which preferentially bind to specific prion strains. Such putative recognition sites could be $PrP^C$ molecules, and regional variation in $PrP^C$ glycosylation could provide a basis for differential strain susceptibility (2, 32, 35). The structural differences between strains are quite substantial, as judged by the strain-specific fluorescence pattern of luminescent polymers (31) or by Fourier transform infrared spectroscopy (8), and may be sufficient in controlling the strength of interactions with differentially expressed cellular ligands/receptors. Second, the efficiencies by which specific neuronal subpopulations are able to propagate different prion strains may vary, possibly because of regional variations in the specificity or activity of chaperones or other putative cofactors. Third, different prion strains could be cleared from different parts of the brain with various efficiencies. Finally, different prion strains may spread transsynaptically to specific regions of the brain at different rates (1). More work is required to distinguish between these various possibilities. Recently, Mahal et al. described an in vitro system that could potentially be exploited to study the molecular basis by which cells preferentially propagate specific prion strains (23). Our current studies show that $PrP^{Sc}$ glycosylation does not play a role in that process.

## ACKNOWLEDGMENTS

We thank Nathan Deleault for helpful discussions and suggestions. We thank Eve Kemble and Michael Miller for help in optimizing and processing the histology slides. We thank David McGuire and Todd Bissonnette for their expert veterinary services.

The National Institutes of Health provided financial support for this study (2R01 NS046478, R01 NS055875, T32 AI007519, and R01 NS049173 to C.S.).

## REFERENCES

1. **Ayers, J. I., A. E. Kincaid, and J. C. Bartz.** 2009. Prion strain targeting independent of strain-specific neuronal tropism. J. Virol. **83:**81–87.
2. **Beringue, V., G. Mallinson, M. Kaisar, M. Tayebi, Z. Sattar, G. Jackson, D. Anstee, J. Collinge, and S. Hawke.** 2003. Regional heterogeneity of cellular prion protein isoforms in the mouse brain. Brain **126:**2065–2073.
3. **Bruce, M. E.** 1993. Scrapie strain variation and mutation. Br. Med. Bull. **49:**822–838.
4. **Carlson, G. A.** 1996. Prion strains. Curr. Top. Microbiol. Immunol. **207:** 35–47.
5. **Carlson, G. A., D. T. Kingsbury, P. A. Goodman, S. Coleman, S. T. Marshall, S. DeArmond, D. Westaway, and S. B. Prusiner.** 1986. Linkage of prion protein and scrapie incubation time genes. Cell **46:**503–511.
6. **Castilla, J., R. Morales, P. Saa, M. Barria, P. Gambetti, and C. Soto.** 2008. Cell-free propagation of prion strains. EMBO J. **27:**2557–2566.
7. **Castilla, J., P. Saa, C. Hetz, and C. Soto.** 2005. In vitro generation of infectious scrapie prions. Cell **121:**195–206.
8. **Caughey, B., G. J. Raymond, and R. A. Bessen.** 1998. Strain-dependent differences in beta-sheet conformations of abnormal prion protein. J. Biol. Chem. **273:**32230–32235.
9. **Collinge, J., K. C. Sidle, J. Meads, J. Ironside, and A. F. Hill.** 1996. Molecular analysis of prion strain variation and the aetiology of 'new variant' CJD. Nature **383:**685–690.
10. **DeArmond, S. J., Y. Qiu, H. Sanchez, P. R. Spilman, A. Ninchak-Casey, D. Alonso, and V. Daggett.** 1999. PrPc glycoform heterogeneity as a function of brain region: implications for selective targeting of neurons by prion strains. J. Neuropathol. Exp. Neurol. **58:**1000–1009.
11. **DeArmond, S. J., H. Sanchez, F. Yehiely, Y. Qiu, A. Ninchak-Casey, V. Daggett, A. P. Camerino, J. Cayetano, M. Rogers, D. Groth, M. Torchia, P. Tremblay, M. R. Scott, F. E. Cohen, and S. B. Prusiner.** 1997. Selective neuronal targeting in prion disease. Neuron **19:**1337–1348.
12. **Deleault, N. R., J. C. Geoghegan, K. Nishina, R. Kascsak, R. A. Williamson, and S. Supattapone.** 2005. Protease-resistant prion protein amplification reconstituted with partially purified substrates and synthetic polyanions. J. Biol. Chem. **280:**26873–26879.
13. **Deleault, N. R., B. T. Harris, J. R. Rees, and S. Supattapone.** 2007. Formation of native prions from minimal components in vitro. Proc. Natl. Acad. Sci. USA **104:**9741–9746.
14. **Endo, T., D. Groth, S. B. Prusiner, and A. Kobata.** 1989. Diversity of oligosaccharide structures linked to asparagines of the scrapie prion protein. Biochemistry **28:**8380–8388.
15. **Ermonval, M., D. Petit, A. Le Duc, O. Kellermann, and P. F. Gallet.** 21 October 2008, posting date. Glycosylation-related genes are variably expressed depending on the differentiation state of a bioaminergic neuronal cell line: implication for the cellular prion protein. Glycoconj. J. doi:10.1007/s10719-008-9198-5
16. **Fraser, H., and A. G. Dickinson.** 1967. Distribution of experimentally induced scrapie lesions in the brain. Nature **216:**1310–1311.
17. **Geoghegan, J. C., P. A. Valdes, N. R. Orem, N. R. Deleault, R. A. Williamson, B. T. Harris, and S. Supattapone.** 2007. Selective incorporation of polyanionic molecules into hamster prions. J. Biol. Chem. **282:**36341–36353.
18. **Glatzel, M., K. Stoeck, H. Seeger, T. Luhrs, and A. Aguzzi.** 2005. Human prion diseases: molecular and clinical aspects. Arch. Neurol. **62:**545–552.
19. **Jones, E. M., and W. K. Surewicz.** 2005. Fibril conformation as the basis of species- and strain-dependent seeding specificity of mammalian prion amyloids. Cell **121:**63–72.
20. **King, C. Y., and R. Diaz-Avalos.** 2004. Protein-only transmission of three yeast prion strains. Nature **428:**319–323.
21. **Levavasseur, E., I. Laffont-Proust, E. Morain, B. A. Faucheux, N. Privat, K. Peoc'h, V. Sazdovitch, J. P. Brandel, J. J. Hauw, and S. Haik.** 2008. Regulating factors of PrP glycosylation in Creutzfeldt-Jakob disease—implications for the dissemination and the diagnosis of human prion strains. PLoS ONE **3:**e2786.
22. **Locht, C., B. Chesebro, R. Race, and J. M. Keith.** 1986. Molecular cloning and complete sequence of prion protein cDNA from mouse brain infected with the scrapie agent. Proc. Natl. Acad. Sci. USA **83:**6372–6376.
23. **Mahal, S. P., C. A. Baker, C. A. Demczyk, E. W. Smith, C. Julius, and C. Weissmann.** 2007. Prion strain discrimination in cell culture: the cell panel assay. Proc. Natl. Acad. Sci. USA **104:**20908–20913.
24. **Makarava, N., and I. V. Baskakov.** 2008. The same primary structure of the prion protein yields two distinct self-propagating states. J. Biol. Chem. **283:** 15988–15996.
25. **Makarava, N., O. V. Bocharova, V. V. Salnikov, L. Breydo, M. Anderson, and I. V. Baskakov.** 2006. Dichotomous versus palm-type mechanisms of lateral assembly of amyloid fibrils. Protein Sci. **15:**1334–1341.
26. **Nishina, K. A., N. R. Deleault, S. P. Mahal, I. Baskakov, T. Luhrs, R. Riek, and S. Supattapone.** 2006. The stoichiometry of host PrPC glycoforms modulates the efficiency of PrPSc formation in vitro. Biochemistry **45:**14129–14139.
27. **Priola, S. A., and V. A. Lawson.** 2001. Glycosylation influences cross-species formation of protease-resistant prion protein. EMBO J. **20:**6692–6699.
28. **Prusiner, S. B.** 1982. Novel proteinaceous infectious particles cause scrapie. Science **216:**136–144.
29. **Prusiner, S. B., S. P. Cochran, D. F. Groth, D. E. Downey, K. A. Bowman, and H. M. Martinez.** 1982. Measurement of the scrapie agent using an incubation time interval assay. Ann. Neurol. **11:**353–358.
30. **Rudd, P. M., M. R. Wormald, D. R. Wing, S. B. Prusiner, and R. A. Dwek.** 2001. Prion glycoprotein: structure, dynamics, and roles for the sugars. Biochemistry **40:**3759–3766.
31. **Sigurdson, C. J., K. P. Nilsson, S. Hornemann, G. Manco, M. Polymenidou, P. Schwarz, M. Leclerc, P. Hammarstrom, K. Wuthrich, and A. Aguzzi.** 2007. Prion strain discrimination using luminescent conjugated polymers. Nat. Methods **4:**1023–1030.
32. **Somerville, R. A., S. Hamilton, and K. Fernie.** 2005. Transmissible spongiform encephalopathy strain, PrP genotype and brain region all affect the degree of glycosylation of PrPSc. J. Gen. Virol. **86:**241–246.
33. **Tanaka, M., P. Chien, N. Naber, R. Cooke, and J. S. Weissman.** 2004. Conformational variations in an infectious protein determine prion strain differences. Nature **428:**323–328.
34. **Tanaka, M., P. Chien, K. Yonekura, and J. S. Weissman.** 2005. Mechanism of cross-species prion transmission: an infectious conformation compatible with two highly divergent yeast prion proteins. Cell **121:**49–62.
35. **Tuzi, N. L., E. Cancellotti, H. Baybutt, L. Blackford, B. Bradford, C. Plinston, A. Coghill, P. Hart, P. Piccardo, R. M. Barron, and J. C. Manson.** 2008. Host PrP glycosylation: a major factor determining the outcome of prion infection. PLoS Biol. **6:**e100.
36. **Vanik, D. L., K. A. Surewicz, and W. K. Surewicz.** 2004. Molecular basis of barriers for interspecies transmissibility of mammalian prions. Mol. Cell **14:**139–145.
37. **Vincent, B., E. Paitel, P. Saftig, Y. Frobert, D. Hartmann, B. De Strooper, J. Grassi, E. Lopez-Perez, and F. Checler.** 2001. The disintegrins ADAM10 and TACE contribute to the constitutive and phorbol ester-regulated normal cleavage of the cellular prion protein. J. Biol. Chem. **276:**37743–37746.
38. **Wang, F., F. Yang, Y. Hu, X. Wang, X. Wang, C. Jin, and J. Ma.** 2007.

Lipid interaction converts prion protein to a PrP(Sc)-like proteinase K-resistant conformation under physiological conditions. Biochemistry **46:**7045–7053.

39. **Wong, C., L. W. Xiong, M. Horiuchi, L. Raymond, K. Wehrly, B. Chesebro, and B. Caughey.** 2001. Sulfated glycans and elevated temperature stimulate PrP(Sc)-dependent cell-free formation of protease-resistant prion protein. EMBO J. **20:**377–386.
40. **Yadavalli, R., R. P. Guttmann, T. Seward, A. P. Centers, R. A. Williamson, and G. C. Telling.** 2004. Calpain-dependent endoproteolytic cleavage of PrPSc modulates scrapie prion propagation. J. Biol. Chem. **279:**21948–21956.
41. **Zuegg, J., and J. E. Gready.** 2000. Molecular dynamics simulation of human prion protein including both N-linked oligosaccharides and the GPI anchor. Glycobiology **10:**959–974.